II. Cesium Leaching in CsA and CsX Zeolites: Use of Blocking Agents to Inhibit the Cesium Cation Mobility

Ilich A. Ibarra,[†] Enrique Lima,*[,†,‡] Sandra Loera,[†] Pedro Bosch,[‡] Silvia Bulbulian,[§] and Victor Lara[†]

Universidad Autónoma Metropolitana, Iztapalapa, A. P. 55-532, Av. San Rafael Atlixco No. 186, 09340 México D.F., México, Instituto de Investigaciones en Materiales, A. P. 70-360, Universidad Nacional Autónoma de México, Circuito Exterior, Ciudad Universitaria, 04510 México D.F., México, and Instituto Nacional de Investigaciones Nucleares, A.P. 18-1027, 11801 México D.F., México

Received: March 28, 2006; In Final Form: August 15, 2006

Cesium-exchanged A and X zeolites were loaded with cesium acetate species and thermally treated in order to inhibit the mobility of exchangeable cesium cations. The proposed procedure seems to block the cavities channels avoiding the releasing of cesium cations under the leaching conditions. The cesium impregnated species did not induce strong structural modifications if they are used in small amounts (0.2 meq/g zeolite), but they promote transformation toward cesium orthosilicate if they are loaded in amounts as high as 2 meq/g zeolite. This orthosilicate retains safely the cesium as it is a component of the lattice.

Introduction

Zeolites are crystalline microporous adsorbents. As they are cationic exchangers, they have been extensively used to remove cationic pollutants from aqueous solutions.[1,2] In 1979, zeolites successfully retained the radioactive cations released[3] in the Three Mile Island accident (57 000 Ci). In 1986, during the Chernobyl disaster, 1 500 000 tons of chabazite were used to trap the radionuclides present in the radioactive wastes.[4] Although radionuclides are easily incorporated into the zeolite network, they may leach out.[5,6] Then, their efficiency to store radioactive materials for long periods remains controversial.

Conventionally, radionuclides containing zeolites are vitrified at high temperatures.[7−9] In this way, radionuclides are safely occluded in the vitreous material and they can be stored for long periods until the radioactivity decays. Vitrified materials may in turn be sensible to radiation or aging developing cracks and defects that could permit lixiviation.[9]

Dyer and Abou-Jamous have proposed to treat radionuclides containing zeolites (^{60}Co, ^{63}Ni, and ^{65}Zn) with a secondary ion-exchange step.[10] A large cation, as barium, may be introduced into the zeolites to block the radioisotope release under leaching conditions. Although these authors observed a minor reduction in isotope release, it was not consistent.

We have shown in our previous work that A and X zeolites are suitable to retain radioactive cesium through cationic exchange.[5] The present work is then focused on how cesium impregnated species can be used to block the zeolite pores and inhibit the cesium cation mobility. In catalytic studies, cesium oxide clusters have been shown to interact strongly with cesium- and sodium-containing zeolites improving the activity in condensation reactions.[11−13]

* To whom correspondence should be addressed. Fax: (525) 58044666. Phone: (525) 58044667. E-mail: lima@xanum.uam.mx.
[†] Universidad Autónoma Metropolitana.
[‡] Universidad Nacional Autónoma de México.
[§] Instituto Nacional de Investigaciones Nucleares.

TABLE 1: Cesium Content in the Impregnated A and X Zeolites as Determined by Nuclear Activation Analyses

exchanged zeolite	volume of added acetate solution (mL)	label	meq Cs/g zeolite
CsX	0.92	CsX-A	1.2
	1.78	CsX-B	1.6
	7.12	CsX-C	2.0
CsA	0.92	CsA-A	1.4
	1.78	CsA-B	1.7
	7.12	CsA-C	2.1

Experimental Methods

Materials. Zeolites NaA and NaX with a framework Si/Al ratio of 1 and 1.2, respectively, were supplied by Union Carbide, type 4A, and Sigma Chemical Company. Other reagents were commercial analytical grade, and they were used without further purification.

Exchange and Impregnation Method. NaA or NaX (5 g) were shaken with 100 mL of 0.1 N $CsNO_3$ solution for 3 h. Then, the solids were separated by centrifugation and washed with deionized water. The exchanged samples are referred in this paper as CsA or CsX.

In a second step, a 0.3 N $CsOOC_2H_3$ solution was dropped on the already cesium exchanged zeolites. The amount of solution was systematically varied, Table 1. After this impregnation, samples were dried at 353 K for 8 h, and calcined at 873 K for 4 h.

Neutron Activation Analysis. The samples were irradiated in a Triga Mark III nuclear reactor for 15 min with an approximate neutron flux of 10^{13} n/cm^2 s. The 0.605 MeV photo peak from ^{134}Cs produced by the nuclear reaction ^{133}Cs (n, γ) ^{134}Cs was measured with a Ge/hyperpure solid-state detector coupled to a computerized 4096-channel pulse analyzer.

X-ray Diffraction (XRD). XRD patterns were obtained in a Siemens D5000 diffractometer, with a wavelength of CuKα. The compounds were identified using the JCPDS files.

Nuclear Magnetic Resonance (NMR) Spectroscopy. The NMR spectra were performed under MAS conditions on a

10.1021/jp061926h CCC: $33.50
Published on Web 10/03/2006

Bruker ASX-300 spectrometer at a resonance frequency of 39.37 MHz for ^{133}Cs. All spectra were recorded after one-pulse excitation with repetition times of 1 s. The spectra were carried out with sample spinning rates of 5 kHz. The chemical shifts were referenced to a 1.0 M aqueous solution of CsCl.

To collect the NMR spectrum data, the samples were prepared and immediately placed in a glovebox under dry N_2. They were, then, packed in ZrO_2 rotors. The time for recording one NMR spectrum was not longer than 10 min.

The ^{27}Al magic angle spinning (MAS) NMR spectra were obtained operating the spectrometer at 78.21 MHz. Pulse width was 2 μs. The spinning rate was 10 kHz. The chemical shift reference was aqueous $[Al(H_2O)_6]^{3+}$.

^{29}Si NMR spectra were obtained at 59.59 MHz by using the combined techniques of MAS and proton dipolar decoupling (HPDEC). Direct pulsed Fourier transform (FT) NMR excitation was used throughout, employing 90° pulses with a pulse repetition time of 8 s. Chemical shifts are expressed as ppm from trimethylsilane.

Xenon gas (Praxair, 99.999%) was used for the ^{129}Xe NMR measurements. For these experiments, the sample powder was placed in a NMR tube equipped with J. Young valves, through which the xenon gas was equilibrated with the sample at 291 K under 1000 Torr of xenon. Prior to xenon loading, samples were dehydrated by gradual heating at 673 K in vacuum (1.33×10^{-4} kPa). ^{129}Xe NMR spectra were recorded at 291 K in a Bruker DMX-500 spectrometer operating at 138.34 MHz. Single excitation pulses were used and at least 5000 scans were collected with a delay time of 2 s. The chemical shift was referenced to xenon gas extrapolated to zero pressure.

Porosity and surface area measurements were performed on a volumetric adsorption autosorb-1 quantachrome apparatus. Prior to adsorption, the samples were outgassed for 12 h at 300 °C. Gas adsorption occurred using nitrogen as the adsorbate at liquid nitrogen temperature (77 K).

Cesium Leaching. Cesium containing zeolites were tested for Cs^+ desorption by shaking them in contact with a 1 N NaCl solution for 2 h. Solids and liquids were then separated by centrifugation, and the desorbed Cs^+ present in the NaCl solution was determined by neutron activation analyses.

Results

Impregnated Cs Zeolites. The content of cesium in each sample, as determined by neutron activation analyses, is reported in Table 1. The exchanged samples contained around 1 meq/g of zeolite (both A and X). After impregnation the amount of cesium was, of course, higher depending on the solution volume.

The XRD patterns of cesium containing samples, impregnated and calcined, are displayed in Figure 1. All observed compounds were crystalline. Nevertheless, it should be emphasized that XRD only detects crystalline compounds when crystallite size is larger than 30 Å and whose content is higher than 3%. Thus, traces of other crystalline or amorphous materials cannot be detected by this technique.

Samples of series A and B maintained the original zeolite structure. No cesium compounds were observed but the crystallinity of samples decreased. In contrast, in the samples loaded with the highest amount of cesium (>2 meq/g), series C, the zeolite peaks faded out, and orthosilicate $CsAlSiO_4$ was identified.

^{133}Cs MAS NMR spectra of samples of both series, CsX and CsA, are presented in Figure 2. The assignment of peaks in the spectra of X zeolites was made as in the works reported by

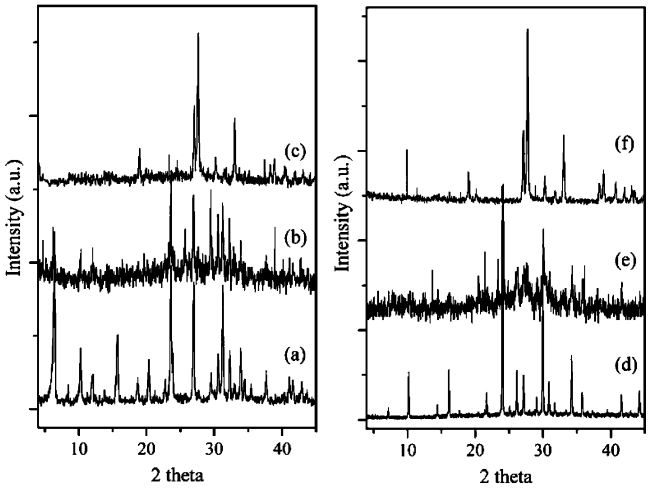

Figure 1. X-ray diffractograms of samples containing cesium CsX-A (a), CsX-B (b), CsX-C (c), CsA-A (d), CsA-B (e), and CsA-C (f).

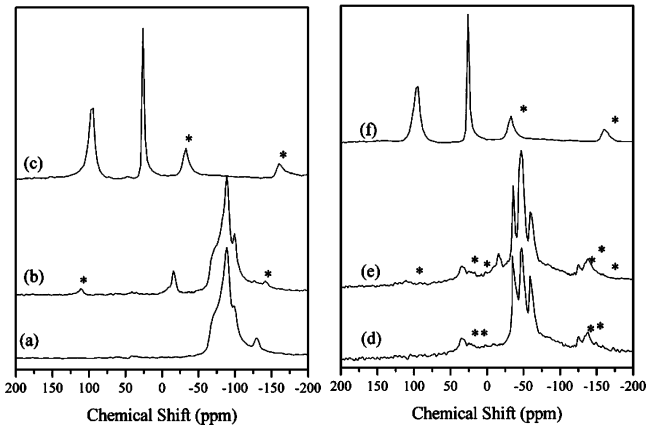

Figure 2. ^{133}Cs MAS NMR spectra of samples containing cesium CsX (a), CsX-B (b), CsX-C (c), CsA (d), CsA-B (e), and CsA-C (f). An asterisk indicates spinning sidebands.

Norby et al.[14] and Hunger et al.[15] In zeolite A no attribution of ^{133}Cs NMR peaks has been reported. Therefore, we assigned the three observed resonances to three different positions of the cations in the zeolite framework as explained in the discussion section.

The impregnated calcined samples (series A and B) presented the resonances due to cesium cations in exchangeable sites and also one signal at −14 ppm was observed (Figure 2). This last one may be attributed to cesium species produced by the thermal treatment of $CsOOC_2H_3$/CsX zeolites. Hereafter, these cesium species are called cesium-impregnated species or simply blocking agents. In samples CsX-C and CsA-C, those with the highest amount of cesium, $CsAlSiO_4$ was identified by XRD and the corresponding ^{133}Cs MAS NMR spectra were constituted by two peaks located at 95 and 22 ppm.

As described by Norby et al.,[14] the relative intensities of the ^{133}Cs NMR peaks may be related to the population of cesium cations in the various exchange sites of the zeolite. Note that signals due to cesium-impregnated species and those due to $CsAlSiO_4$ were resolved from signals corresponding to cesium cations in the exchange positions, Figure 2, Table 2.

Figure 3 shows the ^{27}Al MAS NMR spectra of cesium-containing zeolites. The spectra of samples maintaining the zeolite structure (labeled A and B) exhibited a single peak at 53 ppm, due to tetrahedral aluminum, Al^{IV}.[16] Instead, samples loaded with the highest amount of cesium, where XRD identified

TABLE 2: Distribution of Cesium Cations in the Zeolite Sites as Determined by the Relative Signal Intensities in the ^{133}Cs MAS NMR Spectra (Peaks Due to Cesium-Impregnated Species and $CsAlSiO_4$, if Present, Were Excluded of the Integration)

		cesium population*					cesium population*		
step	sample (FAU)	SIII	SII	SII′	SI′	sample (LTA)	Cs(1)	Cs(2)	Cs(3)
before leaching	CsX	0.40	0.31	0.19	0.10	CsA	0.36	0.35	0.29
	CsX-A	0.43	0.39	0.18		CsA-A	0.40	0.31	0.29
	CsX-B	0.47	0.35	0.18		CsA-B	0.34	0.39	0.27
	CsX-C					CsA-C			
after leaching	CsX	0.34	0.28	0.24	0.14	CsA	0.33	0.34	0.33
	CsX-A	0.46	0.33	0.21		CsA-A	0.37	0.33	0.30
	CsX-B	0.45	0.36	0.19		CsA-B	0.34	0.35	0.31
	CsX-C					CsA-C			

$CsAlSiO_4$, aluminum remained tetrahedrally coordinated, but the peak appeared at 57 ppm and it was clearly narrower than the zeolite corresponding one.

We turn now to the N_2 isotherms in Figure 4. The nitrogen isotherms for X zeolite series are significantly altered as the cesium-impregnated species are present. The isotherm on samples maintaining the zeolite structure, CsX-A and CsX-B samples, show isotherms concave to the p/po axis, then it follows a trend almost linear and, finally, is convex to the p/po axis. In contrast, the isotherm on the sample CsX-C is convex to the p/po axis over the full range. This feature is indicative of weak adsorbent−adsorbate interactions.

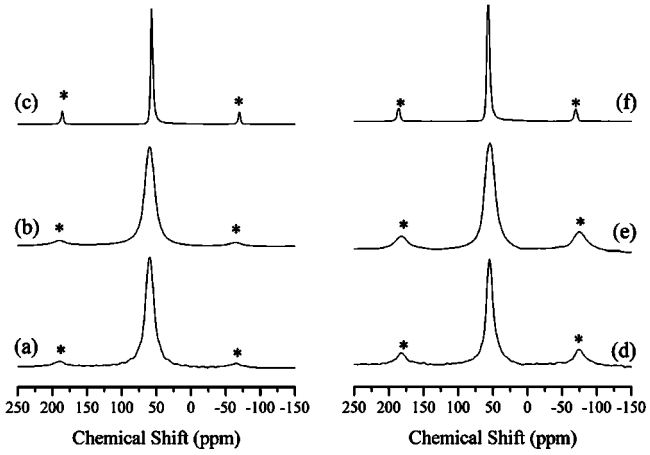

Figure 3. ^{27}Al MAS NMR spectra of samples CsX (a), CsX-B (b), CsX-C (c), CsA (d), CsA-B (e), and CsA-C (f). An asterisk indicates spinning sidebands (spinning rate 10 kHz).

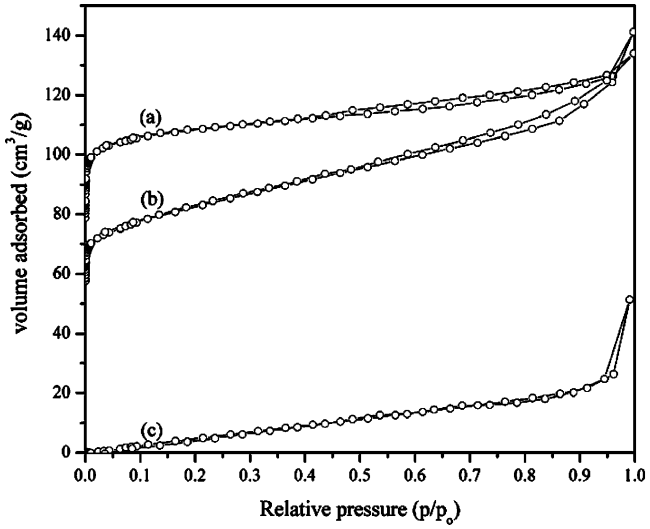

Figure 4. N_2 adsorption−desorption isotherms at 77 K on CsX-A (a), CsX-B (b), and CsX-C (c) samples.

TABLE 3: Surface Specific Area, Total Pore Volume, and Pore Size in CsX Series

code sample	specific surface area[a] (m^2/g)	total pore volume[a] (cm^3/g)	average pore diameter[b] (Å)
CsX	601	0.32	21
CsX-A	309	0.23	26
CsX-B	250	0.19	34
CsX-C	36	0.08	87

[a] Calculated from N_2 adsorption−desorption isotherms and the Brunauer−Emmett−Teller method. [b] From N_2 adsorption−desorption isotherms and the Barrett−Joyner−Halenda method.

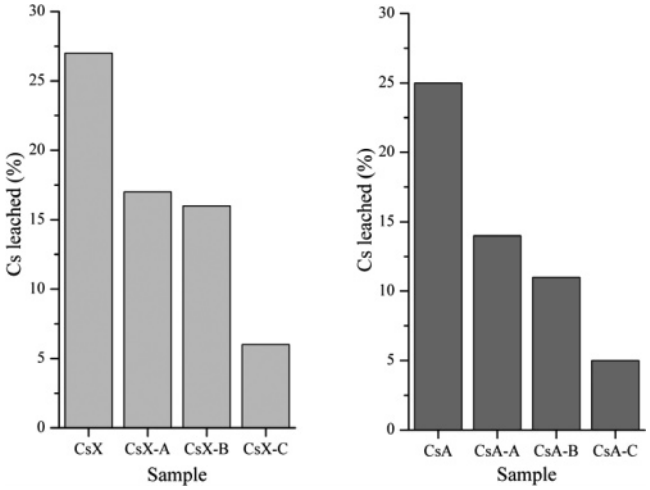

Figure 5. Leached cesium in the different samples, (light gray) series X and (dark gray) series A. Concentration of blocking agents (cesium oxide species) increases from left to right in both histograms. Sample CsX is free of cesium oxide.

The specific surfaces areas as determined by the BET method, the pore size and the pore volume of the samples are included in Table 3.

Leaching Out Tests. Histograms in Figure 5 compare the percentage of cesium leached in the various calcined solids after contact with the sodium solution. For comparison purposes, the results of samples without blocking agents (samples CsX and CsA), were also included. The observed trend is similar in the two types of zeolite: before impregnation, i.e., when the samples were free of cesium-impregnated species, samples leached as much as 25%. In samples of series A and B, the amount of leached cesium decreased down to 5%.

Similar distributions of cesium cations, as determined by ^{133}Cs NMR, were found in the samples, before and after leaching tests, Table 2. As mentioned above, in some of the samples the signals due to blocking agents or $CsAlSiO_4$ were present. The ^{133}Cs NMR signals for these compounds also remained unaltered after the leaching step.

As expected, ^{27}Al MAS NMR spectra did not vary after the leaching tests.

SCHEME 1

$$2CsOOC_2H_3 + 4O_2 \longrightarrow Cs_2O + 3\,H_2O + 4\,CO_2$$

Leaching tests did not alter the crystalline lattice as no differences were observed in the XRD patterns, leached or nonleached samples.

Discussion

Nonleached Samples. XRD results show that the incorporation of cesium-impregnated species does induce changes in the crystallinity of zeolites from series A and B. The XRD peaks of cesium oxide or any other cesium compound formed upon the thermal decomposition of the cesium acetate were not observed. Neither the NMR is able to propose the chemical nature of these cesium-impregnated species. Laspéras et al.[12] have suggested that impregnation of cesium acetate on zeolites CsX and subsequent thermal treatment leads to cesium oxide loaded into zeolitic cavities. However, it should be mentioned that cesium oxide, as other alkaline oxides, can react with water to produce hydroxide species. From the data presented in this work it is difficult to disclose between oxide or hydroxide species. Assuming that cesium acetate could decompose to form oxide, the amount of cesium oxide formed in our samples of series A and B could be close to 0. 2 wt %, Scheme 1, which is beyond the detection limits of the XRD technique. On the contrary, in the solids with the highest cesium loading, zeolite structures faded out and the aluminosilicate $CsAlSiO_4$ was formed. It is worth mentioning that $CsAlSiO_4$, with a Si/Al ratio of 1, was obtained from A zeolite as well as from X zeolite. Zeolite A has a Si/Al ratio of 1 but not the X zeolite whose molar ratio is higher (1.2). Then, in the CsX-C sample some amount of siliceous material remains undetected by XRD. In this sense, the ^{29}Si MAS NMR spectra are more illustrative as they show the Si(*n*Al) units which build the zeolite framework, where *n* is the number of aluminums bonded to tetrahedral silicon $(SiO_4)^{4-}$. From Figure 6 it can be stated that cesium X zeolites are built by Si(4Al), Si(3Al), Si(2Al), Si(1Al), and Si(0Al) units, signals at −84, −88, −93, −98, and −102, respectively.[17] Furthermore, from relative intensities ($I_{Si(nAl)}$) in the corresponding spectra and under the Lowenstein rule, which says that Al−O−Al bonds are forbidden, the Si/Al ratio was determined for the zeolite samples,[18,19] according to

$$\frac{Si}{Al} = \frac{\sum_{n=0}^{4} I_{Si(nAl)}}{\sum_{n=0}^{4} 0.25 n I_{Si(nAl)}}$$

The Si/Al ratio was maintained equal to 1.2; hence, with the presence of cesium-impregnated species the zeolites were not dealuminated. When the zeolite was loaded with an amount of cesium as high as 2 meq/g, series C, the zeolite structure turned out to be $CsAlSiO_4$, which is an aluminosilicate composed only by Si(2Al) units, signal at −93 ppm. In the case of cesium-containing A zeolites, the ^{29}Si MAS NMR spectra show only one resonance, which has been controversially assigned to Si(3Al) units; however, it is now usually agreed that this peak must be assigned to Si(4Al) units,[20−22] i.e., the framework is ordered and built by Si(4Al) units which became Si(2Al) units in the sample CsA-C where $CsAlSiO_4$ was formed. In both groups of zeolites, CsA and CsX, Si(4Al) units are transformed to Si(2Al), as represented in Scheme 2. This conclusion is further

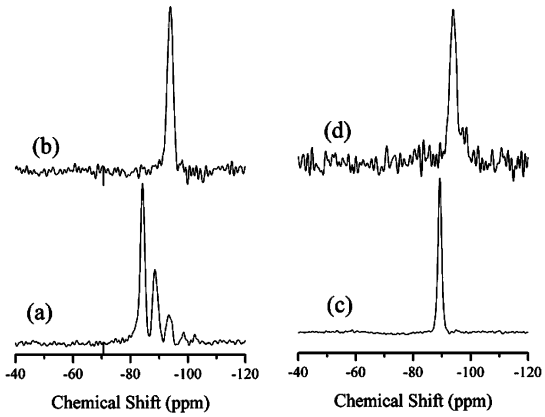

Figure 6. ^{29}Si MAS NMR spectra of samples: CsX-B (a), CsX-C (b), CsA-B (c), and CsA-C (d).

SCHEME 2

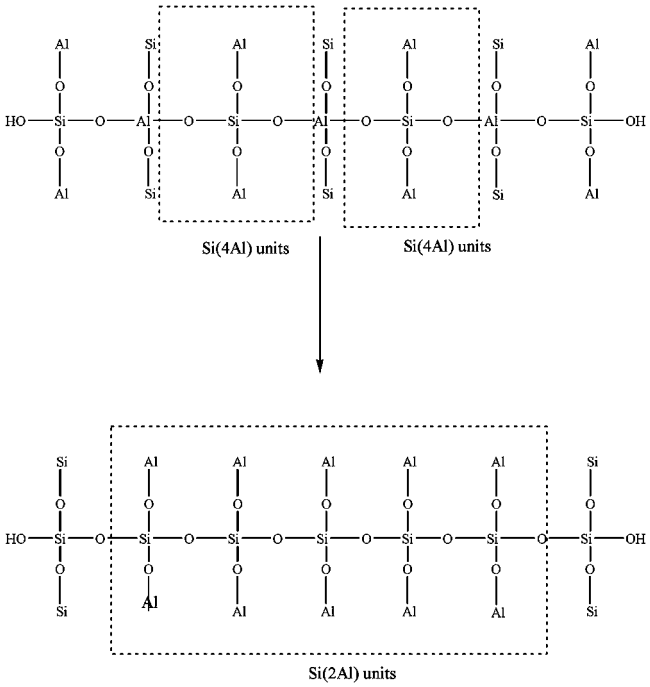

supported by the ^{27}Al NMR results, which show that aluminum remains tetrahedrally coordinated.

From the ^{133}Cs MAS NMR results, cesium distribution, in the various exchangeable cation sites of the zeolite framework, may be obtained. However, the first task is the attribution of the peaks in the ^{133}Cs NMR spectra of the A zeolites. The exchangeable cations can occupy three different sites in zeolite A:[23,24] cations can be located on the 4, 6, and 8 rings, Figure 7. If it is assumed that cesium may be positioned without rearrangement of the rings; then 3 resonances should be observed in the ^{133}Cs NMR spectra. Furthermore, in zeolite A,

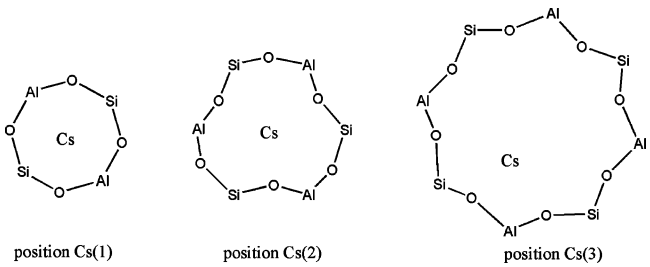

Figure 7. Cation positions on rings in zeolite CsA.

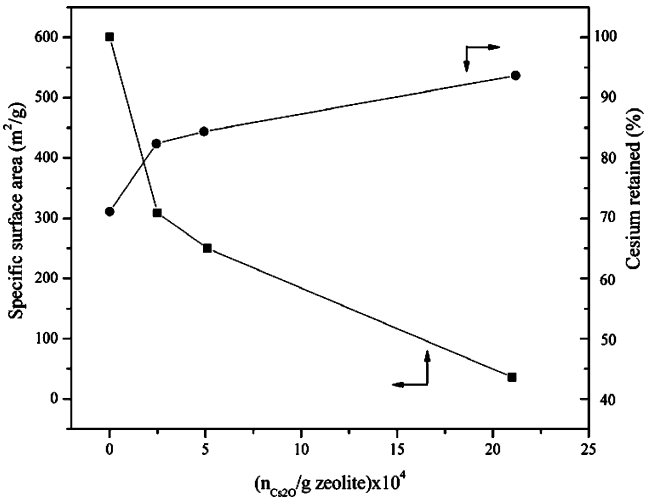

Figure 8. Cesium retention and specific surface area as a function of the cesium oxide loaded in the Cs-X series.

which has a Si/Al ratio of 1 with a full alternation of Al and Si, each 4R has two aluminums, two silicons, and four oxygens, and similarly for the 6R and 8R units. In these cases, all framework oxygens have the same formal contribution to Si and Al atoms on a simple electrostatic model. Then, the charge on the exchangeable cations is determined by the number of the oxygen atoms surrounding it. As the number of oxygen atoms neighboring the cesium cations increases, the resonance peak should be shifted to stronger fields. Then, the resonances of cesium cations in positions Cs(1), Cs(2), and Cs(3) of Figure 7 can be ordered from higher to lower resonance field as follows: Cs(3) > Cs(2) > Cs(1). In the spectra included in Figure 2, the peaks observed at −60.3, −45.7, and −35 ppm may be attributed to cesium cations in positions Cs(3), Cs(2), and Cs(1), respectively. It has to be emphasized that these signals are resolved from those attributed to cesium oxide and $CsAlSiO_4$. Then the distribution of Cs^+ in CsA samples can be determined, Table 3. From this table a conclusion emerges: When zeolites contain blocking agents, the mobility of Cs^+ as compensating cation is significantly inhibited. Indeed, in the X zeolite, free of blocking agents, the cations are distributed 71% in the large cavity and 29% in the sodalite cages. In contrast, when cesium-impregnated species are present, only 18% of Cs^+ reaches the sodalite cages. In the A zeolite, Cs^+ has a similar distribution in samples free or loaded with cesium oxide species.

The N_2 adsorption−desorption isotherms are more useful to explain the inhibition in cesium mobility. In isotherms on samples CsX-A and CsX-B the called point B is clearly resolved. However, the knee of the isotherm became sharp as blocking agents increases. The ordinate of point B gives an estimation of the amount of adsorbate required to cover the unit mass of solid surface with a complete monomolecular layer. Note that the amount of adsorbate as well as the specific surface area and pore volume diminish as the amount of blocking agent increases, Table 3. A conclusion can be drawn from this result: The porous material turns out to be denser. The isotherm on sample where no more zeolite was detected, sample CsX-C, corresponds to a nonporous material confirming the conclusion cited above.

^{133}Cs spectra of samples identified as cesium orthosilicate presented two peaks with similar intensities but with very different line width. The resonance at weak field was broader than the resonance at high field. From Ashbrook et al.,[25] both resonances are due to cesium orthosilicate. The corresponding ^{27}Al MAS NMR spectra exhibited a single symmetrical peak confirming that the system is ordered and that quadrupole interactions are minimized.

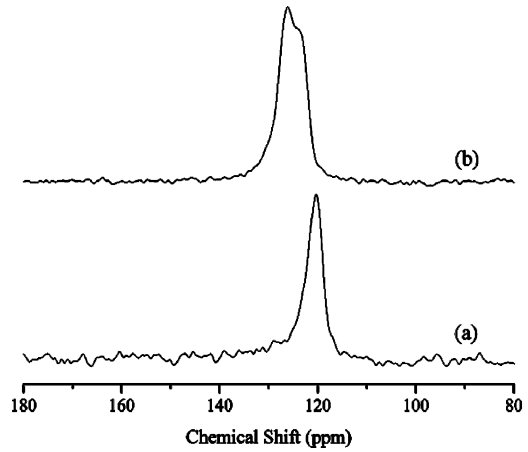

Figure 9. ^{129}Xe NMR spectra of xenon adsorbed (P_{Xe} = 1000 Torr) on CsX (a) and CsX-A (b) samples.

Leached Samples. The amount of cesium-impregnated species can be expressed as Cs_2O. Thus, the amount of cesium retained may be plotted as a function of Cs_2O content, Figure 8. If samples containing cesium oxide species are compared with the samples free of cesium impregnated species a clear effect of these species on cesium retention (as Cs^+) is observed. The concentrations of Cs_2O proposed in this work promote the introduction of blocking agents species into the zeolite cavities, reducing the free space and inhibiting the mobility of cesium cations. To disclose the diffusion of cesium impregnated species into the zeolitic cavities, two ^{129}Xe NMR spectra were recorded, Figure 9. The spectrum for CsX sample is composed for a single peak at 120 ppm which agrees with results reported for cesium exchanged faujasites.[26] On the contrary, spectrum for CsX-A sample exhibits two peaks at higher chemical shifts indicating that cesium-impregnated species are heterogeneously distributed inside the large cavities.[27,28] The diameter of xenon is 0.43 nm, then it cannot enter to sodalite cages and it is a probe molecule selective for the large cavities.

The clearest effect of loading zeolites with cesium species by impregnation is the loss of porous network as shown by nitrogen adsorption study. Figure 8 reveals that cesium retention increases as the blocking agents concentration augments, the specific surface area evolves in an opposite way. It is clear that the blocking agents induce, in samples CsX-A and CsX-B, modest structural changes not detected by DRX and promoting denser materials. If cesium-impregnated species concentration is too high, $CsAlSiO_4$ is produced as the zeolite network is destroyed, cesium is not anymore retained or blocked as a cation into the cavities of zeolites. Instead, it is stabilized as a component of the cesium orthosilicate lattice.

The very similar distribution of cesium cations, before and after the leaching step, confirms that cation mobility is strongly reduced by the presence of the cesium oxide and, even, the water is not able to change the distribution of cations, as shown previously for samples thermally treated, free of cesium-impregnated species.[5]

Conclusion

The impregnation of cesium-exchanged zeolites with cesium acetate and a further thermal treatment produces complex solids where cesium oxide and exchanged cesium zeolite are in close interaction. In these solids the exchanged cesium in the large

cavities of the zeolite does not leach out. Still cesium remains confined in the large cavity and does not reach the sodalite cages.

With high loading of cesium oxide, the structure of the exchanged zeolite is destroyed and cesium orthosilicate is formed. As cesium is incorporated into the lattice of this compound, it is not released.

Acknowledgment. The technical work of Marco Antonio Vera and Alejandro Montesinos (UAMI) is gratefully acknowledged.

References and Notes

(1) Kalló, D. *Application of natural zeolites in water and wastewater treatments*; M. D. W., Bish D. L., Eds.; The Mineralogical Society of America: Washington, U.S.A. 2001.

(2) Yu, J.-S.; Kevan, L. *J. Phys. Chem.* **1991**, *95*, 3262.

(3) Roskill. *Zeolites Economy*, 1st ed.; Information Services Ltd.: 1988.

(4) Pansini, M. *Mineral. Dep.* **1996**, *31*, 563.

(5) Lima, E. J.; Ibarra, I. A.; Vera, M. A.; Lara, V. H.; Bosch, P.; Bulbulian, S. *J. Phys. Chem. B* **2004**, *108*, 12103.

(6) Al-Attar, L.; Dyer, A.; Harjula, R. J. *J. Radioanal. Nucl. Chem.* **2004**, *260*, 199.

(7) Thamzil, L. *Waste treatment immobilization technologies involving inorganic sorbents*; International Atomic Energy Agency: Vienna, 1997.

(8) Bulbulian, S.; Bosch, P. *J. Nucl. Mater.* **2001**, *295*, 64.

(9) Lima, E. J.; Lara, V. H.; Bulbulian, S.; Bosch, P. *Chem. Mater.* **2004**, *16*, 2255.

(10) Dyer, A.; Abou-Jamous, J. K. *J. Radioanal. Nucl. Chem.* **1997**, *224*, 59.

(11) Hathaway, P. E.; Davis, M. E. *J. Catal.* **1989**, *116*, 263.

(12) Laspéras, M.; Cambon, H.; Brunel, D.; Rodriguez, I.; Geneste, P. *Micro. Mater.* **1996**, *7*, 61.

(13) Lima, E.; Ménorval, L.-C. D.; Laspéras, M.; Eckhard, J. F.; Graffin, P.; Tichit, D.; Fajula, F. *Stud. Surf. Sci. Catal.* **2001**, *135*, 232.

(14) Norby, P.; Poshni, F. I.; Gualtieri, A. F.; Hanson, J. C.; Grey, C. P. *J. Phys. Chem. B* **1998**, *102*, 839.

(15) Hunger, M.; Schenk, U.; Burger, B.; Weitkamp, J. *Angew. Chem., Int. Ed. Engl.* **1977**, *36*, 2504.

(16) Fyfe, C. A.; Gobbi, G. C.; Kennedy, G. J.; Graham, J. D.; Ozubko, R. S.; Murphy, W. J.; Bothner, A.; Dadok, J.; Chesnick, A. S. *Zeolites* **1985**, *5*, 179.

(17) Lippmaa, E.; Magi, M.; Samoson, A.; Engelhardt, G.; Grimmer, A. R. *J. Am. Chem. Soc.* **1980**, *102*, 4889.

(18) Lippmaa, E.; Magi, M.; Samoson, A.; Tarmac, M.; Engelhardt, G. *J. Am. Chem. Soc.* **1981**, *103*, 4992.

(19) Loewenstein, W. *Am. Mineral.* **1954**, *39*, 92.

(20) Newsam, J. M. *J. Phys. Chem.* **1987**, *5*, 91.

(21) Klinowski, J.; Thomas, J. M.; Fyfe, C. A.; Hartman, J. S. *J. Phys. Chem.* **1981**, *85*, 2590.

(22) Dimitrijevic, R.; Dondur, V. *J. Solid State* **1995**, *115*, 214.

(23) Breck, D. W. *Zeolite molecular sieves*; J. Wiley Sons: New York, 1974.

(24) Pluth, J. J.; Smith, J. V. *J. Am. Chem. Soc.* **1980**, *102*, 4704.

(25) Ashbrook, S. E.; Whittle, K. R.; Polles, L. L.; Farnan, I, *J. Am. Ceram. Soc.* **2005**, *88*, 1575.

(26) Liu, S.-B.; Fung, B. M.; Yang, T.-C.; Hong, E.-C.; Chang, C. T.; Shih, P.-C.; Tong, F.-H.; Chen, T.-L. *J. Phys. Chem. B* **1994**, *98*, 4393.

(27) Guillemot, D.; Borokov, V. Y.; Kazansky, V. B.; Polisset-Thfoin, M. P.; Fraissard, J. *J. Chem. Soc., Faraday Trans.* **1997**, *93*, 3587.

(28) Menorval, L. C. D.; Fraissard, J.; Ito, T.; Primet, M. *J. Chem. Soc., Faraday Trans. 1* **1985**, *81*, 2855.